Supplementary information

PtCu alloy cocatalysts for efficient photocatalytic CO_2 reduction into CH_4 with 100% selectivity

Junyi Wang, Youzi Li, Jiangting Zhao, Zhuo Xiong*, Yongchun Zhao*, Junying Zhang

State Key Laboratory of Coal Combustion, School of Energy and Power Engineering, Huazhong University of Science and Technology, Wuhan 430074, China

*Corresponding authors: Tel:+862787542417; Email: zxiong@hust.edu.cn; yczhao@hust.edu.cn

Catalyst preparation

TiO_2 catalysts with different Pt/Cu ratios were synthesized by a H_2-reduction method. The specific process is as follows: firstly, 0.1g TiO_2 powder (P25) was dispersed in 50 ml of a mixed solution of H_2PtCl_6 and Cu $(NO_3)_2$ and vigorously stirred for 30 minutes and the mass ratio of metal to TiO_2 is 1%. Then place the mixed solution in a constant temperature water bath at 80 °C with stirring until the solution was completely evaporated to dryness. The obtained solid powder was calcined in a muffle furnace at 450 °C under air atmosphere for 2h, and then reduced at 450 °C under 20% H_2/N_2 atmosphere in tubular furnace for 2h to obtain the required samples. All samples are labeled as TiO_2-PtxCuy (x and y represent the proportion of Pt and Cu, respectively, with x + y=1, x=0, 0.2, 0.4, 0.6, 0.8, 1).

Catalyst characterization

X-ray diffraction (XRD) patterns were recorded on X'Pert PROX diffractometer from

PANalytical B.V. of the Netherlands. The surface area and porosity were measured by a Micrometrics analyzer (ASAP 2020) through N_2 adsorption-desorption. The concentration of Pt in the catalysts was measured by inductively coupled plasma-optical emission spectrometry (ICP-OES) using an Agilent ICP-OES instrument. Transmission electron microscopy (TEM) images were obtained by using the 44 Talos F200X instrument produced by the Dutch FEI company. The electron-hole recombination characteristics were obtained from photoluminescence (PL) spectra with excitation by a 325 nm laser using a LabRAM HR800c focal laser Raman microscope. The UV-Vis diffuse reflectance spectrum (DRS) of the samples was measured by Shimadzu's 46 SolidSpec-3700 UV-Vis near-infrared spectrophotometer. The surface atomic composition of the catalysts and the chemical states of Pt were recorded by a Thermo Scientific Escalab 250Xi X-ray photoelectron spectroscopy (XPS). Photoluminescence (PL) spectroscopy were performed on a confocal laser LabRAM HR800 instrument using a 325 nm excitation light source. QuantaMaster 8000 fluorescence spectrometer (HORIBA, CANADA) was employed to record TRPL spectra. Temperature programmed CO_2/CO desorption (CO_2/CO-TPD) measurements were conducted on a ChemiSorb 2720 instrument.

All the PEC measurements were carried out using a standard three-electrode electrochemical workstation (CHI770E) composed of a Pt foil as the counter electrode, ITO coated with the catalyst as the working electrode, and Ag/AgCl as the reference electrode. A 300W Xe lamp equipped with an AM1.5 filter was used as irradiation source with a radiometer. 0.5 M Na_2SO_4 aqueous solution was employed as electrode.

Photocurrent density measurements as a function of time (J-t) with on and off cycles were carried out at a fixed bias of 0 V vs. Ag/AgCl. Electrochemical impedance spectroscopy (EIS) measurements were conducted with an amplitude of 5 mV over a frequency ranging from 0.01 to 100 kHz. The in situ Fourier transform infrared (FTIR) spectroscopy were collected on a Nicolet iS50 spectrometer (Thermofisher). Thein situ experiments were conducted in a Harrick reaction chamber with two ZnSe windows and another quartz window, which are used for IR and UV light transmission, respectively.

Photocatalytic reduction of CO_2

The CO_2 photocatalytic reduction reaction system consists of a water bath system, a self-made reactor, a 300 W Xenon lamp source (Microsolar300, Beijing Perfectlight) equipped with UV filter (300 nm < λ < 400 nm), and an online gas chromatography (GC). The top of the reactor is piece of quartz glass, and the Xe lamp is located about 10 cm above the reactor. Before the illumination, the reactor was first purged with a mixture of CO_2 and water vapor at a flow rate of 300 mL/min for 1 h, in order to purify the air in the reactor, and then switched to a stable flow rate of 10 mL/min for 30 min, then the light source was turned on to irradiate a Petri plate containing 20 mg of catalyst. The reactor was closed in a constant temperature system, maintaining the temperature at 30 °C. During the 4-hour light irradiation, gaseous reaction mixtures containing CO, CH_4, H_2 and O_2 will be analyzed using a gas chromatograph equipped with a TCD, FID and a methanizer. The GC used argon (≥99.999%) as the carrier gas and was equipped with two packed columns (TDX-01 and Molsieve 5 Å) and two gas switching valves in the back channel. During the

analysis, a 1.0 mL gas sample was introduced through the sample loop into the TDX-01 column, where the CO_2 was separated from the other gases due to its long retention time. The remaining gases are further separated by a Molsieve 5 Å column. H_2 and O_2 are detected by TCD and due to the sensitivity limitations of TCD, traces of H_2 may not be detected as they do not reach the lower detection limit. CH_4 and CO are detected by FID with higher sensitivity. The function of the methanizer is to convert CO to CH_4 for FID analysis. During the reaction of CO_2 photoreduction, there may be traces of liquid products such as CH_3OH, HCOOH and HCHO that may not be detected as the corresponding column is not configured.

The apparent quantum yield (AQY) of the photocatalytic reaction system was evaluated using a light source with 365 nm monochromatic light. The irradiated area for the photocatalytic reaction was controlled as the circle with diameter of 4 cm. The AQY and the carbon-based selectivity for the carbon-containing products were calculated according to the following equations:

$$AQY(\%) = \frac{Number\ of\ reacted\ electrons}{Number\ of\ incident\ photos} \times 100 = \frac{2n_{CO} + 8n_{CH_4}}{n_{photons}} \times 100$$

$$S_{CH_4}(\%) = \frac{n_{CH_4}}{n_{CO} + n_{CH_4}} \times 100$$

Blank experiments were performed to identify that all carbon-containing products measured by GC originated from high purity purged CO_2. First, a mixture of CO_2 and H_2O vapor was used as the reactants in the empty reactor or reactor with only a Petri plate in it. The results showed that, in the above two cases, no carbon-containing products were

generated in the dark or under light, indicating that the CO_2 reduction reaction would not occur without photocatalyst. In addition, CO_2 was replaced with N_2 and passed to the reaction system, and no hydrocarbon was detected under the same conditions. The above tests confirmed that all carbon-containing products are derived from high-purity carbon dioxide.

Density functional theory calculation method

All plane-wave density functional theory (DFT)[1-2] calculations were performed using the Vienna Ab initio Simulation Package (VASP).[3-4] The vdW-DF functional was used for the exchange-correlation energy.[5-6] The Kohn–Sham one-electron valence states were expanded in a basis of plane waves with energy cutoff of 450 eV. The Pt, Cu, PtCu surfaces were modeled as a five−layer slab using p(2x2) unit cells, in which a vacuum layer of 15 Å in the z direction was applied to avoid the interaction between layers and the top three layers was allowed to relax. For all slab calculations, the Brillouin zones were sampled with 3 × 3 × 1 Monkhorst-Pack grids.[7] Convergence with the force on each atom was set below 0.04 eV/Å and the energy on each atom was within 1×10^{-4} eV for all geometry optimization and 1×10^{-5} eV for all the zero-point energies calculation. To evaluate the thermodynamic stability of the different slabs, Gibbs free energies, ΔG (298.15 K), were obtained by combining the electronic and zero−point energies with enthalpy and entropy corrections from frequency calculations. PBE frequencies were used to compute the Gibbs free energies.[8] The free energy of CO_2 photoreduction steps were calculated using the following equation: $\Delta G = \Delta E + \Delta E_{ZPE} - T\Delta S$, where the ΔE, ΔE_{ZPE}, and ΔS are

electronic energy, zero-point energy, and entropy difference between products and reactants.

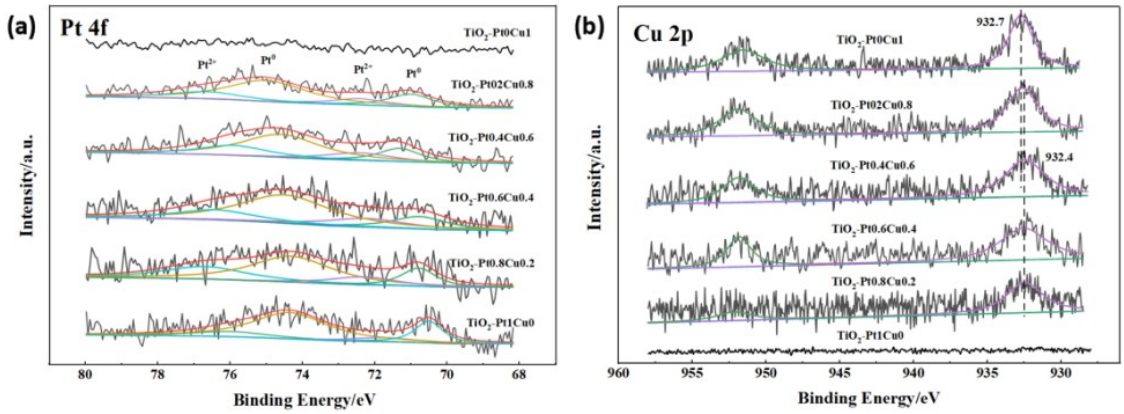

Fig. S1 XPS spectra of a) Pt 4f and b) Cu 2p of TiO_2-PtxCuy.

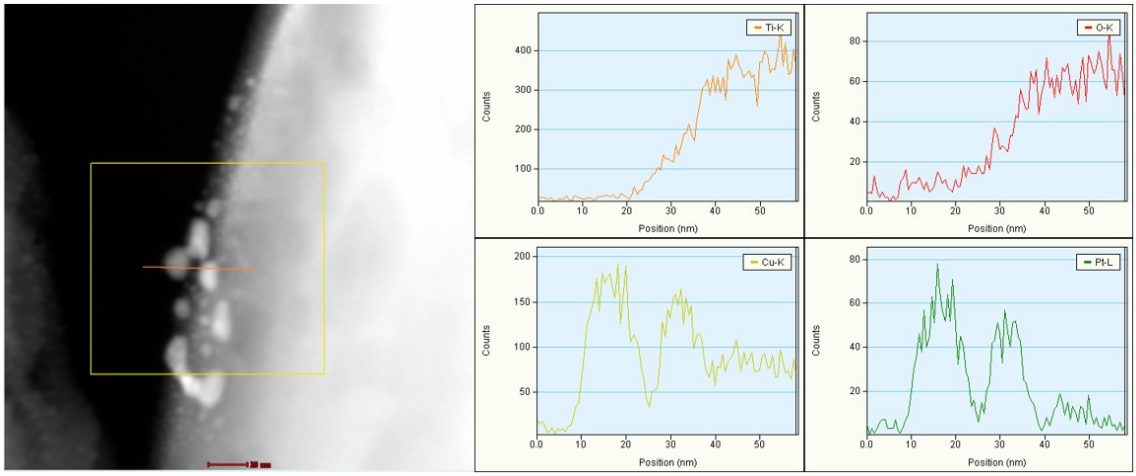

Fig. S2 HAADF-STEM image and EDS line scan of TiO_2-Pt0.4Cu0.6.

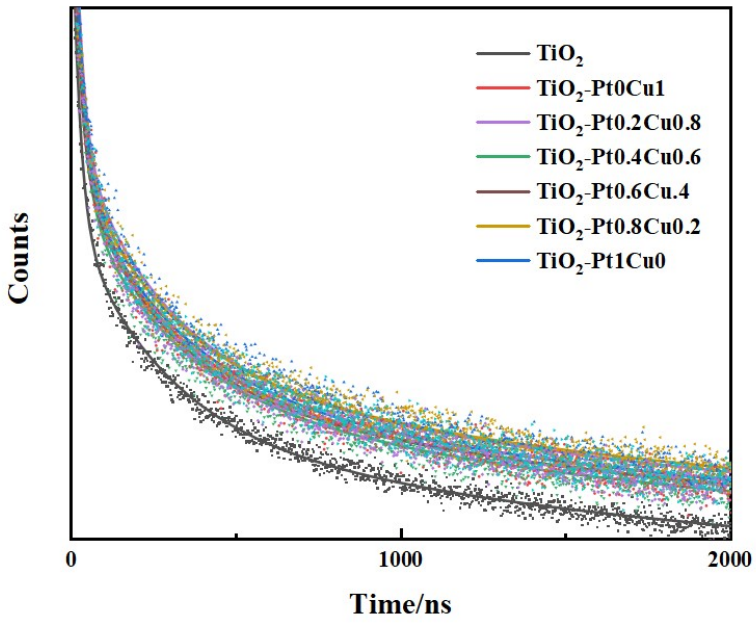

Fig. S3 TRPL spectrum of TiO_2-PtxCuy.

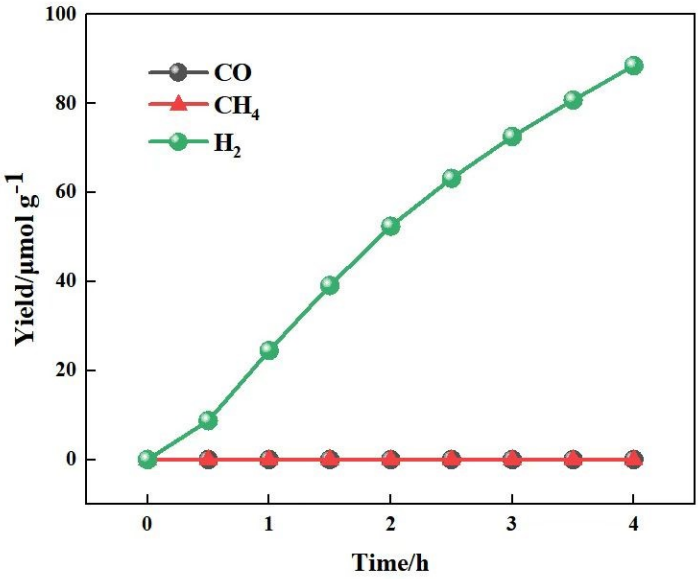

Fig. S4 Production yields of water-splitting experiment over TiO_2-Pt1Cu0.

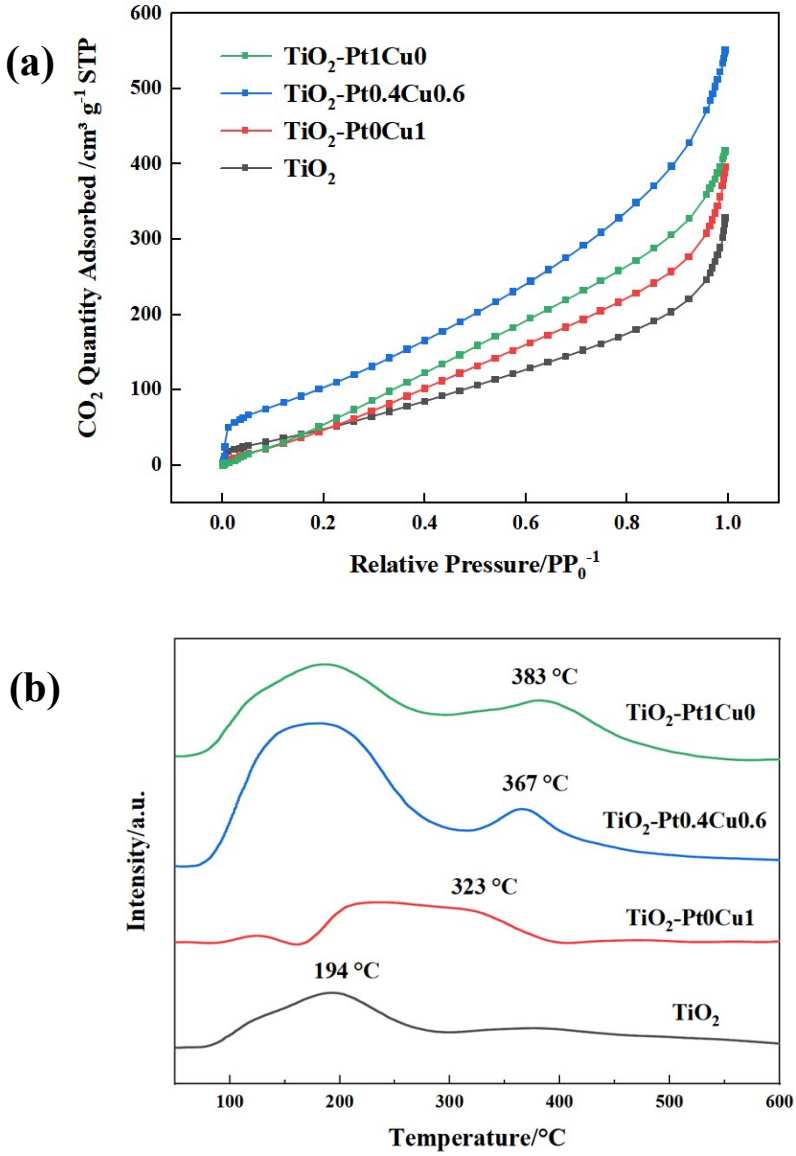

Fig. S5 a) CO_2 adsorption isotherms and b) CO_2-TPD of TiO_2-PtxCuy.

Table S1 AQY and CH_4 selectivity of TiO_2-PtxCuy.

Samples	Apparent Quantum Yield	CH_4 Selectivity
TiO_2	0.09%	18.7%
TiO_2-Pt0Cu1	0.17%	20.1%
TiO_2-Pt0.2Cu0.8	0.18%	73.1%
TiO_2-Pt0.4Cu0.6	**0.56%**	**100%**
TiO_2-Pt0.6Cu0.4	0.28%	100%
TiO_2-Pt0.8Cu0.2	0.20%	100%
TiO_2-Pt1Cu0	0.18%	100%

Table S2 metal alloy cocatalysts for CO_2 photoreduction.

Photocatalyst	Cocatalyst	Light source	Loading method	Reaction medium	Main product	Selectivity of main product	Ref.
$SrTiO_3/TiO_2$	Au_3Cu	300 W Xe lamp	Microwave-assisted solvothermal	33.3% CO_2 and $N_2H_4 \cdot H_2O$	CO	83.7%	[9]
TiO_2 NWs	Ag/Au	35W HID Xe	Chemical and photoreduction	CO_2 and H_2	CO	97.7%	[10]
TiO_2 NCs	Au_6Pd_1	300 W Xe lamp	Photoreduction	CO_2 and H_2O	CH_4	71%	[11]
TiO_2	AuCu	1000 W Xe lamp	stepwise deposition–precipitation	CO_2 and H_2O vapor	CH_4	93.5%	[12]
TiO_2	PtRu	300 W Xe lamp 320 nm - 780 nm	P-GBMR	CO_2 and H_2O	CH_4	93.7%	[13]
TiO_2 NSs	Pd_7Cu_1	300 W Xe lamp ＜400 nm	Aqueous solution	CO_2 and H_2O	CH_4	95.9%	[14]
TiO_2	PtCu	300 W Xe lamp 300 nm - 400 nm	H_2-reduction	CO_2 and H_2O vapor	CH_4	100%	In this work

References

[1] P. Hohenberg; W. Kohn, Physical Review 136 (1964) B864-B871.

[2] W. Kohn; L.J. Sham, Physical Review 140 (1965) A1133-A1138.

[3] G. Kresse; J. Furthmüller, Physical Review B 54 (1996) 11169-11186.

[4] G. Kresse; J. Furthmüller, Computational Materials Science 6 (1996) 15-50.

[5] M. Dion; H. Rydberg; E. Schröder; D.C. Langreth; B.I. Lundqvist, Physical Review Letters 92 (2004) 246401.

[6] J. Klimeš; D.R. Bowler; A. Michaelides, Physical Review B 83 (2011) 195131.

[7] H.J. Monkhorst; J.D. Pack, Physical Review B 13 (1976) 5188-5192.

[8] J.P. Perdew; K. Burke; M. Ernzerhof, Physical Review Letters 77 (1996) 3865-3868.

[9] Q. Kang; T. Wang; P. Li; L. Liu; K. Chang; M. Li; J. Ye, Angewandte Chemie International Edition 54 (2015) 841-845.

[10] M. Tahir; B. Tahir; N.a.S. Amin, Applied Catalysis B: Environmental 204 (2017) 548-560.

[11] Q. Chen; X. Chen; M. Fang; J. Chen; Y. Li; Z. Xie; Q. Kuang; L. Zheng, Journal of Materials Chemistry A 7 (2019) 1334-1340.

[12] Ş. Neaţu; J.A. Maciá-Agulló; P. Concepción; H. Garcia, Journal of the American Chemical Society 136 (2014) 15969-15976.

[13] Y. Wei; X. Wu; Y. Zhao; L. Wang; Z. Zhao; X. Huang; J. Liu; J. Li, Applied Catalysis B: Environmental 236 (2018) 445-457.

[14] R. Long; Y. Li; Y. Liu; S. Chen; X. Zheng; C. Gao; C. He; N. Chen; Z. Qi; L. Song; J. Jiang; J. Zhu; Y. Xiong, Journal of the American Chemical Society 139 (2017) 4486-4492.